Low-Diffusivity Lattice-Gas Models of Mixtures

by

Richard T. Holme

B.A., Physics and Theoretical Physics,
Cambridge University
(1989)

Submitted to the Department of
Earth, Atmospheric, and Planetary Sciences
in partial fulfillment of the requirements for the degree of

Master of Science in Geophysics

at the

MASSACHUSETTS INSTITUTE OF TECHNOLOGY

February 1991

Author .....
Department of Earth, Atmospheric, and Planetary Sciences
January 18th, 1991

Certified by .....
Daniel H. Rothman
Associate Professor of Geophysics
Thesis Supervisor

Accepted by ....
Thomas H. Jordan
Department Head
Department of Earth, Atmospheric, and Planetary Sciences

Low-Diffusivity Lattice-Gas Models of Mixtures

by

Richard T. Holme

Submitted to the Department of Earth, Atmospheric, and Planetary Sciences
on January 18th, 1991, in partial fulfillment of the
requirements for the degree of
Master of Science in Geophysics

Abstract

I develop lattice-gas and lattice-Boltzmann models for the study of mixing in low diffusivity systems. Previous work in this area has focused on lattice-gas models with local interactions. I extend this to a lattice-gas model with non-local interactions. I also introduce a two phase lattice-Boltzmann model with local interactions, based on a linearised collision operator, and then combine these techniques to produce a non-local lattice-Boltzmann model.

The non-local lattice-gas model is designed to preserve interfaces between multiple phase systems. It is demonstrated to have a lower diffusivity than existing models. Random fluctuations caused by the discrete nature of the algorithm produce non-equilibrium behaviour which is likely to make the model inefficient for much numerical work. However, it could have specialised applications in studying phase separation and anomalous diffusion.

Theory is developed for a lattice-Boltzmann model for two-phase fluids with only local interactions. Diffusivity is shown to depend on a particular eigenvalue of the linearised collision matrix. Numerical studies confirm the analytical result. Diffusivity can be achieved which is close, but not arbitrarily close, to zero. This method will be applicable to studies of low diffusivity systems in which interfacial interactions are unimportant.

A non-local lattice-Boltzmann model is outlined, using ideas from the two previous models. This is used to lower the diffusivity achievable using the local model. Further studies are necessary to determine this model's usefulness.

Thesis Supervisor: Daniel H. Rothman
Title: Associate Professor of Geophysics

ACKNOWLEDGMENTS

Much of this work was performed while I held tenure as a Kennedy scholar. I would like to express my gratitude to the Kennedy Memorial Trust and its Board of Trustees, whose generosity enabled me to undertake this project. Computing hardware and other group facilities were provided through grants from the sponsors of the MIT Porous Flow Project. I am extremely grateful to Professor Dan Rotham for his constant interest in and assistance with my work, particularly towards its conclusion. Finally, I would like to thank Andrew Gunstensen for frequent help with technical problems, his excellent code and graphics routines, and his tolerance of a rather unbalanced lab mate.

Contents

List of Figures

Chapter 1

Introduction

The scope of this thesis is to develop lattice-gas and lattice-Boltzmann techniques for investigation of mixing in low diffusivity systems. I construct a new lattice-gas algorithm to achieve integrity of interfaces over long time periods without interfacial forces. I formulate established models in terms of a linearised lattice-Boltzmann algorithm to investigate the stability of such methods at very low diffusivities, and then I combine the two approaches to produce a model that is computationally clean and may extend the lower bound on achievable diffusivities. Each of these models exhibits features which are difficult to achieve using standard lattice methods.

Low diffusivity systems are of broad scientific, and in particular geophysical, interest. Relevant problems exist in many diverse areas of study. Lattice-gas and lattice-Boltzmann techniques have already been successfully applied to studies of flow in porous media [1, 2], and multiphase systems [3, 4]. Study of dispersion in porous media [5] may be possible, in particular anomalous diffusion, which is characterised by an apparent effective diffusivity that grows with length scale. Many unresolved problems in mantle dynamics depend on the mixing dynamics of physical and chemical heterogeneities resulting from, or even causing, mantle convection [6]. Similar problems are encountered in core dynamics, where the motion of such heterogeneities may drive the geodynamo [7]. Analytical techniques are not powerful enough, and

laboratory experiments cannot achieve the parameter ranges required, to model such systems.

LATTICE GASES

Lattice-gas dynamics is a fundamentally different computational tool for the study of fluid dynamics and other systems governed by related partial differential equations. Lattice gas models are a form of cellular automata. Standard models have particles of uniform mass moving on a periodic lattice, usually with uniform speed, interacting at the lattice nodes. The algorithm is intrinsically discrete in space, time and physical units. Interactions, usually described as collisions, typically depend only on conditions (the state) at that site or at nearest neighbours. The models can be deterministic (one to one) or probabilistic. They have received much attention due to their computational advantages. As no discretisation is necessary implementation on computer is easy, and the local evolution lends itself to massively parallel processing. While models have been developed to study a wide variety of physical situations, particular success has come in two areas of fluid dynamics: flow through porous media and multiple-phase flow. The former has proved fruitful as lattice gases can simulate arbitrarily complex geometries with negligible computational cost, while the latter enables easy tracking of interfaces, a process that can be troublesome with traditional numerical methods such as finite-element techniques.

While earlier work exists in the literature, widespread study of lattice-gas models began relatively recently. An early lattice-gas model was due to Hardy, de Pazzis and Pomeau [8], since referred to as the HPP model. Particles move on a square, two dimensional lattice and scatter with deterministic rules conserving total particle number (mass) and linear momentum. Collision rules are chosen so as to define transport coefficients, for example viscosity. The macroscopic behaviour is close to the 2D Navier Stokes equations for fluid flow, but includes anisotropy which affects the viscosity. This is avoided by turning instead to a class of models introduced by

Frisch, Hasslacher and Pomeau [9], now known as FHP lattice-gases. They are based on a two dimensional hexagonal lattice, which has sufficient symmetry to achieve isotropy in transport properties. This issue is discussed in reference [10].

2D work has focused on variants of two types of FHP model. FHP I type have six allowed states per site, one for each direction of the lattice, while FHP II type add an extra rest particle (zero velocity) as an allowed state. This allows a greater variety of possible collisions, and so more control over transport properties. In all cases, no more than one particle is allowed in each state. The background to these models, and the derivation of the macroscopic behaviour, is discussed more fully in references [10, 11].

No three dimensional lattice exists that correctly satisfies the symmetry requirements if restricted to unit mass particles. It is necessary to include a fourth dimension, use a face centred hypercubic lattice, and then collapse the extra direction. Such lattices have been named FCHC [12].

In all cases, the time evolution of the model can be divided into two parts: propagation, when particles move from one lattice node to the next, and collision, when they interact.

Study of two-phase models has been fruitful. The particles of an FHP model are "coloured" to make them distinguishable, by convention "red" and "blue". They can then represent two different fluids with distinct properties. Many systems can be modeled in this way. For example, if the total colour is allowed to vary in a particular way, the macroscopic behaviour can represent certain types of chemical reaction [13]. More commonly, total particle colour is conserved so as to describe the interaction of inert fluids. By choice of appropriate rules, different viscosities [14, 15] and diffusivities [16] can be modeled, while applying non local rules has allowed the simulation of interfacial forces [17] and the liquid gas transition [18].

While systems have been studied with more than two types of particle (for example [19]), most work has focused on two-phase flow. Only such two component systems

will be considered here. Colouring means there are now two aspects to the collision: the particles must still be arranged to conserve mass and momentum, and colour must be redistributed. We can define two collision types: those in which the physical outcome depends on the colour of the particles, and those in which the colour is rearranged as a passive tracer, with the motion of the particles unchanged from an uncoloured system. Collision rules and recolouring rules can be chosen so as to allow considerable variation in transport properties. I shall restrict my attention to considering ways to minimise the diffusivity.

Previous work in this area has focused on purely local collision rules, in which the outcome of a collision depends only on the occupancy of that site. An example of such a model is the so called "limited diffusion" model introduced by D'Humières and others [16]. However, work begun by Rothman and Keller [17] suggested an attractive alternative. These workers used a non-local collision algorithm, where the updating of a site depends on the states of other nodes, to determine the outcome of a collision. Specifically, they reorganised the particle directions so that, given conservation of colour and momentum, they maximised particle motion towards regions of like colour. With this approach, they were able to simulate interfacial forces which caused complete phase separation into homogeneous regions with stable interfaces. The efficiency of the separation suggested that an algorithm based on a similar approach but without producing interfacial forces could result in a very low diffusivity model. This is investigated in Chapter 2.

LATTICE-BOLTZMANN TECHNIQUES

Some of the advantages of lattice-gas methods have already been mentioned. There are also certain significant problems. The discrete nature of the model leads to a high level of statistical noise. For many purposes, this means that massive, computationally expensive, spatial and temporal averaging is required to obtain clean results. Recently, an attractive alternative has emerged. Instead of considering the evolution

of a system of particles, we consider the evolution of mean population density, using a Boltzmann approximation that the states are uncorrelated [20, 21]. This eliminates much of the need for averaging as the results are implicitly the mean outcome. Two approaches are possible - either to use a full representation of the collision operator [20], or to linearise about a local equilibrium [21]. I will follow the latter approach.

In Chapter 3, I derive the linearised Boltzmann operator for a two colour system, analogous to the established low-diffusivity algorithms, and demonstrate that the diffusivity is determined by a particular eigenvalue of the operator. From this numerical experiments are performed to investigate its minimisation. Chapter 4 is in some sense an fusion of the results of the previous two chapters. It details the application of a Boltzmann method to the algorithm developed in Chapter 2. Chapter 5 briefly discusses possible future avenues of investigation.

Chapter 2

A Virtually-Immiscible Lattice Gas

Low-diffusivity two phase lattice gases have previously been extensively studied (see, for example, [16]). I present a new approach to achieving low diffusivity, closely related to the ILG model of Rothman and Keller [17], which achieves two fluid immiscibility by simulating interfacial tension. In both the ILG and the new model, local colour gradient is measured and a new state selected to be aligned with that gradient. I aim to produce a model with a diffusivity sufficiently low that interfaces are maintained for long time periods. Hence, separation of the two phases is to be maintained without interfacial forces. I shall subsequently refer to this condition as the fluids being virtually immiscible, as on the time scale of interest the two phases are to remain unmixed.

MODEL

Our study was conducted using a variant of an FHP II lattice gas, described previously. To reiterate, this consists of a hexagonal lattice occupied by particles of equal mass which either have speed of one lattice unit per time step or are stationary. An exclusion principle applies such that each site has an allowed occupancy of 7 parti-

cles; one particle with each of the six possible velocities and one rest particle. As in previous studies, a two phase system is defined by giving each particle an additional property, described as "colour". I follow convention by referring to these as red and blue. The colour of a given particle is unchanged during the lattice dynamics.

I shall use the following notation. The ith velocity vector is denoted by $\mathbf{c}_i$; $\mathbf{c}_0 = \mathbf{0}$ and $\mathbf{c}_1$ through $\mathbf{c}_6$ are unit vectors connecting neighbouring sites on the triangular lattice. The Boolean variables $r_i(\mathbf{x}) \in \{0,1\}$ and $b_i(\mathbf{x}) \in \{0,1\}$ indicate the presence or absence of a red or blue particle with velocity $\mathbf{c}_i$ at lattice site $\mathbf{x}$. The configuration at a site is thus completely described by the two 7-bit variables $r = \{r_i, i = 0,\ldots,6\}$ and $b = \{b_i, i = 0,\ldots,6\}$. Colour is only a label attached to a particle: thus there may be only one particle in any given state, and this particle may be either red or blue.

The outcome of a collision, $r \rightarrow r''$, $b \rightarrow b''$, is determined as a two stage process, via an intermediate state (r', b'). Firstly, the configuration is chosen at random from those satisfying the constraints of coloured mass conservation

$$\sum_i r'_i = \sum_i r_i, \qquad \sum_i b'_i = \sum_i b_i, \tag{2.1}$$

and colourblind momentum conservation

$$\sum_i \mathbf{c}_i(r'_i + b'_i) = \sum_i \mathbf{c}_i(r_i + b_i). \tag{2.2}$$

Then, given this new mass distribution, the colour is rearranged so as to align the coloured velocities with the local colour gradient. This can be expressed mathematically as follows. I define the local colour flux to be the difference between the net red momentum and net blue momentum at site $\mathbf{x}$:

$$\mathbf{q}[r(\mathbf{x}), b(\mathbf{x})] \equiv \sum_i \mathbf{c}_i[r_i(\mathbf{x}) - b_i(\mathbf{x})]. \tag{2.3}$$

The local colour field $\mathbf{f}(\mathbf{x})$ is defined to be to be the vectorial sum of the differences between the number of reds and the number of blues at neighbouring sites [i.e., the

microscopic gradient of the signed (red minus blue) colour density]:

$$\mathbf{f}(\mathbf{x}) \equiv \sum_i \mathbf{c}_i \sum_j [r_j(\mathbf{x}+\mathbf{c}_i) - b_j(\mathbf{x}+\mathbf{c}_i)]. \tag{2.4}$$

We seek to maximise the projection of the colour flux in the direction of the colour field,

$$\mathbf{f} \cdot \mathbf{q}(r'', b''). \tag{2.5}$$

The occupancy of a state is unchanged - this step merely swaps the colours of the particles. This can be written, for each i,

$$r_i'' + b_i'' = r_i' + b_i'. \tag{2.6}$$

If there is more than one outcome for either stage of the collision process that satisfies the requirements equally well, the result is decided by random selection from those outcomes.

In the study of Rothman and Keller, the rearrangement of the colour is performed simultaneously with the collision. The colour field affects the particle dynamics, generating the interfacial forces that the model was designed to simulate. My model was designed to achieve virtually-immiscible fluids on the basis of low diffusion, rather than surface tension. Eliminating the interfacial forces by splitting the collision into a two stage process means that the particles at each site are rearranged less efficiently than as part of a one step process, because the state occupancy is determined at random rather than in order to align the particles most effectively. Thus the separation will be less effective.

Once the collisions have been calculated, each particle moves one lattice unit in its direction of motion. The effect of the collisions will be to cause this to be towards regions containing particles predominantly of the same colour.

CHARACTERISATION OF MODEL DIFFUSIVITY

A number of different methods have been used by previous workers to characterise diffusivity, including studies of random walk processes and relaxation of a colour

density step [16]. Influenced by the non-equilibrium properties described below, I chose to use a scheme similar to that described by McNamara [22], measuring flow of colour driven by a steady state linear colour gradient. A rectangular channel, 64x128 lattice units in size, was set up with a boundary at each of the short sides and toroidal boundary conditions relating the long sides. Reflections from the boundary were calculated using free slip boundary conditions, but also included a recolouring step, such that all the particles hitting at one end had their colour changed to red, while all those at the other end were changed to blue. This created a linear colour gradient between the ends of the channel. The colour field of the system then evolves according to the diffusion equation:

$$\partial_t \sigma + \partial_i(\sigma v_i) = \partial_i(D(d)\partial_i \sigma) \tag{2.7}$$

where d is the reduced mass density, defined as number of particles per state, D is the diffusivity, and $\sigma = d_{red} - d_{blue}$ is the difference between the coloured mass densities. If particle velocities and occupancies can be assumed to be uncorrelated, this reduces to the standard linear diffusion equation:

$$\partial_t \sigma = D(d)\nabla^2 \sigma \tag{2.8}$$

Under such conditions, the macroscopic flux of colour can be expected to be directly proportional to the colour density gradient. Here density is defined per unit area rather than per lattice site. This can be expressed as Fick's law:

$$\mathbf{J}_\sigma = -D\nabla\phi \tag{2.9}$$

Here $\mathbf{J}$ is the flux of colour through a line per unit length, and ϕ is the colour density. Thus the ratio of colour flux to colour gradient yields the diffusion coefficient [23].

Simulations were performed over 100,000 time steps. The lattice was sampled only after 50,000 steps to ensure that full equilibrium had been achieved. I sampled every 250 steps subsequently, with averaging being performed over channel width and time, within half of the lattice away from the boundary walls. This eliminated edge

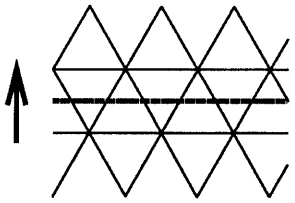

FIG. 2-1. Schematic of line through which flux is measured. Arrow represents direction of colour gradient.

effects. Colour gradient was calculated using a least squares fit, with an eyeball check to confirm an equilibrium gradient, and flux in the channel determined by adding vectorially the flow of the particles across lines between the lattice in this region (shown in Figure 2-1) and averaging. This provides a good value for the average flux per unit area crossing a line in the lattice at any given point.

Diffusivity was measured for three different collision algorithms - colourblind, limited diffusion and the new algorithm. The colourblind model is called self-diffusion by D'Humieres - particles are rearranged without reference to colour, and then colour is randomly assigned within the resulting configuration. The limited diffusion model maximises the change in momentum for each coloured species. Hence, the reorientation depends only on the state of a particular site and not on its surrounding colour field. This approach achieves a reduced diffusivity but with no integrity of interfaces.

A comparison of measured diffusivities is presented as Figure 2-2. The data for the established algorithms show good agreement with previous work [16]. Unsurprisingly, both models with optimised collisions exhibit lower diffusivity than the self-diffusion model. At very low densities, the limited diffusion algorithm is superior to the new model, but at density 0.2 and above, the new model is clearly better. This can be explained by the difference in optimisation methods. Diffusivity has been defined above as related to the ratio of flux to the global colour gradient. The two methods sample this gradient imperfectly: limiting the measurement to one site only with the limited diffusion model, and to the six nearest neighbours with the new model. Clearly at high densities the latter will provide the better approximation. At lower

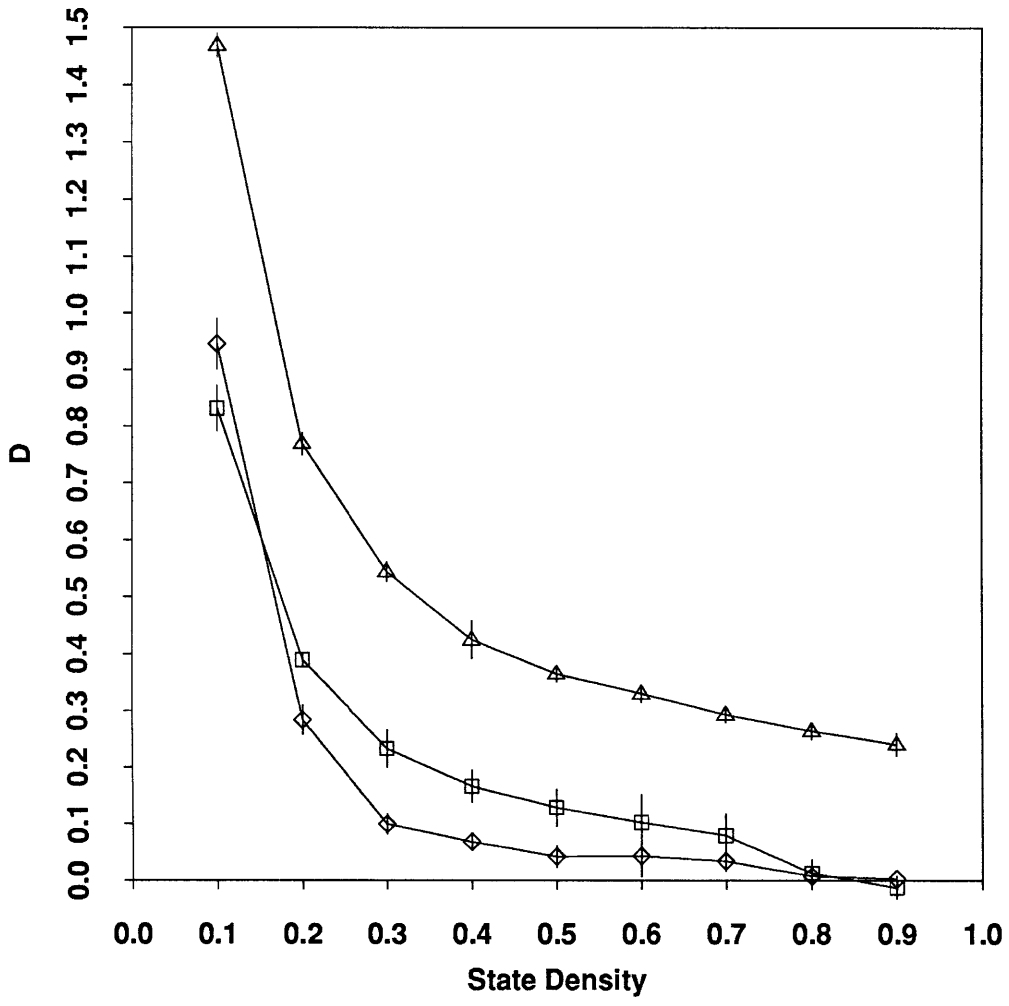

FIG. 2-2. Comparison of diffusion coefficients for different models

◇ New algorithm

□ Limited Diffusion

△ Colourblind

Error bars are at the 1σ level

densities, sites where a valid collision can occur are rare, and the population around them will be sparse. Thus it is likely that in such a case, the local colour field will not be well defined, and be highly susceptible to random fluctuations. The new algorithm will not operate effectively, whereas the efficiency of the limited diffusion model is unchanged.

A comment is necessary on the reproducibility of measurements. Error bars are shown for the 1σ level of confidence, with a sample size of order 10. Errors are larger at higher densities for the optimised rules, as clumping (non equilibrium behaviour) occurs, introducing non-linearities into the colour profile. This is particularly severe for the new algorithm.

NON-EQUILIBRIUM PROPERTIES

The algorithm was originally constructed as an attempt to limit mixing with no interfacial forces. This is achieved. However, random fluctuations of the interface allow "fingering", and when these fingers become sufficiently thin at the point of attachment (again by random fluctuations) they can become detached. Two initially homogeneous regions gradually disintegrate into many small bubbles. This is shown in Figure 2-3. An initially random distribution of particles approaches the same equilibrium. Thus the long term equilibrium state for the algorithm consists of a mixture of bubbles of fluid, constantly decomposing, changing morphology and reconnecting. The characteristic size of these particles is an increasing function of density, and for example is about 5 lattice units at density 0.7. The bulk diffusion rate measured by experiment is for the diffusion of these blobs, likely to be different from the diffusion of individual particles. I postulate that this is some form of Brownian process.

The equilibrium time for these bubbles to form completely is long (of the order of 10^4 time steps), sufficient to allow simulation of various features previously achieved with the ILG (for example Rayleigh-Taylor and Kelvin-Helmholtz instabilities).

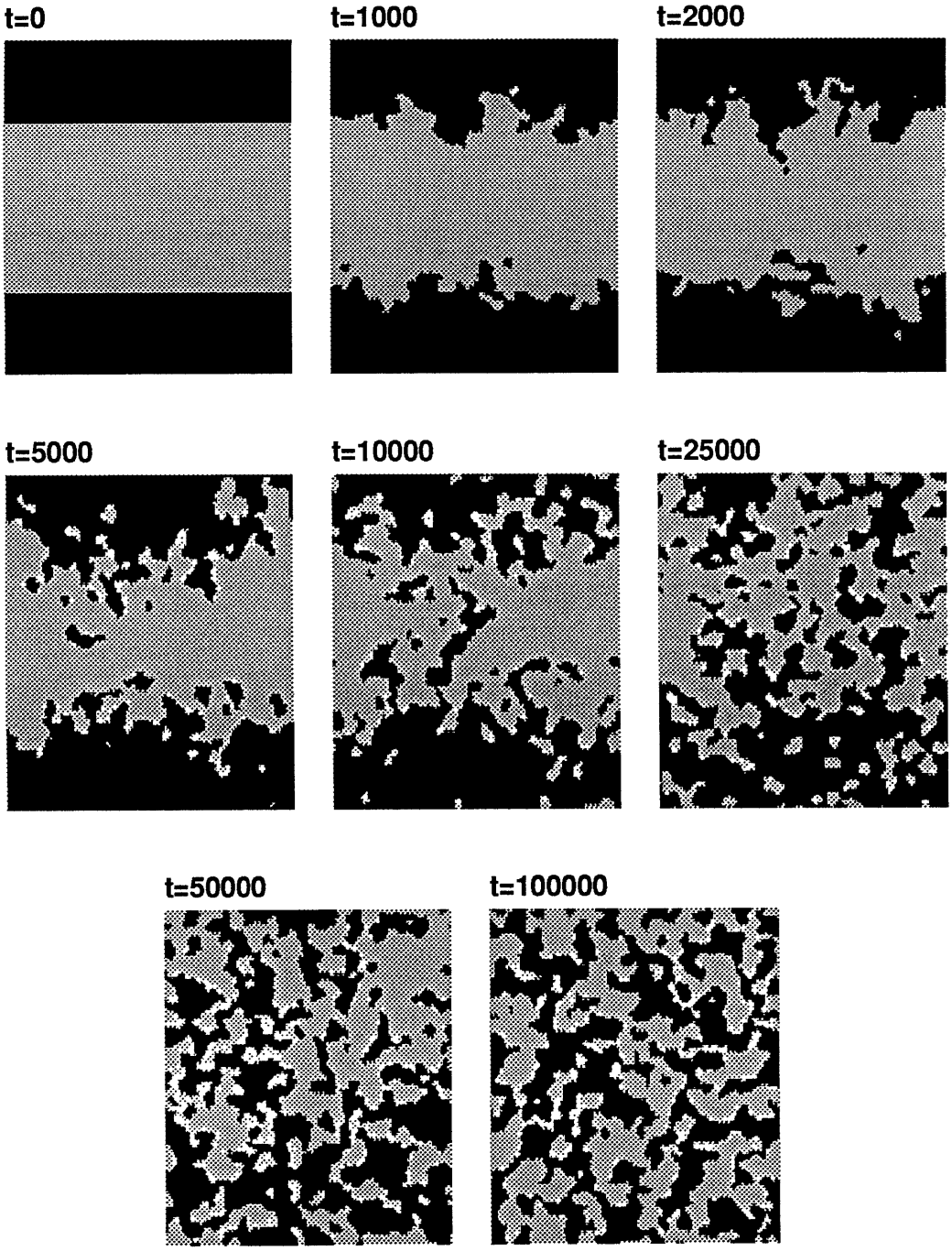

FIG. 2-3. Non-equilibrium behaviour of model

APPLICATIONS

This model has been shown to exhibit a reduced diffusivity, and to maintain the integrity of interfaces on a short time scale. However, the non-equilibrium properties of the model described above seem to make it inappropriate for many forms of numerical work. For most initial and boundary conditions, the lattice undergoes a transition from the initial state in which the lattice dynamics is dominated by interactions between single particles, to a state where the dynamics are controlled by the interactions of bubbles. These clusters provide the characteristic microscale for large times, thus multiplying the lattice dimensions necessary for simulations by a factor of five or so. Computation times become too great for sensible studies (lattice areas must be increased by well over an order of magnitude, and a considerable number of time steps must be initially set aside for equilibrium to be achieved).

One possible area of application for the model is the study of anomalous diffusion, mentioned in Chapter 1. The multiple microscales seem a possible approach to the modeling of scale dependent diffusion.

Many of the problems can be eliminated by utilising the lattice-Boltzmann counterpart of this model. This is discussed further in Chapter 4.

Chapter 3

Derivation of a Local Two Colour Linearised Collision Operator

INTRODUCTION

This chapter has three sections. Firstly, the existence of a local two colour linearised collision operator is motivated by examining the lattice-gas collision operator in the limit of the Boltzmann approximation. Secondly, the operator is generalised as far as possible and an eigenvalue associated with the diffusivity of the system is isolated. Thirdly, numerical studies are detailed which confirm this theory.

MOTIVATION OF A TWO COLOUR LINEARISED COLLISION OPERATOR

To simplify the mathematical development, I consider an FHP I type model, thus excluding rest particles. The state at a lattice site is defined by a set of 12 Boolean variables:

$$s = (r_1, b_1, r_2, b_2, \ldots, r_6, b_6), \tag{3.1}$$

where r_i is 1 if there is a red particle present travelling in direction i and 0 otherwise. Adopting the standard exclusion principle, no more than one particle per state is

allowed: r_i and b_i cannot simultaneously be 1. An output state is defined similarly:

$$s' = (r'_1, b'_1, r'_2, b'_2, \ldots, r'_6, b'_6). \tag{3.2}$$

The two states are linked by a collision - a rearrangement of the particles at the site given certain conservation laws. The primed notation indicates a state following collision and prior to propagation. We write the probability of state s becoming state s' as $A(s; s')$. Clearly the sum of all the output probabilities for a given input configuration must be 1, thus

$$\sum_{s'} A(s; s') = 1. \tag{3.3}$$

We assume that this relation is symmetric, so that

$$\sum_{s} A(s; s') = 1. \tag{3.4}$$

This is called the principal of semi detailed balance. Further discussion of the consequences of this and a proof for the FHP lattice can be found in [10].

I adopt standard conservation rules for collisions. For non zero collision probability A, conservation of coloured mass yields

$$p'_r = \sum_i r'_i = p_r = \sum_i r_i, \qquad p'_b = \sum_i b'_i = p_b = \sum_i b_i, \tag{3.5}$$

where p_r and p_b are the number of red and blue particles at the site. Momentum conservation gives

$$\sum_i \mathbf{c}_i(r'_i + b'_i) = \sum_i \mathbf{c}_i(r_i + b_i). \tag{3.6}$$

Following a simplified version of the scheme adopted by Rothman and Zaleski [24], I assume use of a Boltzmann approximation is valid. This is based on a molecular chaos postulate [25], that the states at each site are uncorrelated, and thus the n-particle distribution functions which characterise the probability of a given state can be written as the product of n one particle distribution functions. Previous work has shown that this is generally a good approximation [25, 22]. Evolution of the model then proceeds by the Boltzmann equation [26].

Thus, the occurrence probability of an input state s is given by

$$\prod_{j=1}^{6} R_j^{r_j}(\mathbf{x},t)B_j^{b_j}(\mathbf{x},t)[1-N_j(\mathbf{x},t)]^{1-r_j-b_j}, \tag{3.7}$$

and the probabilities of having particles of each colour with a given velocity in the output state is

$$\begin{aligned} R_i' &= \textstyle\sum_{s,s'} r_i' A \prod_{j=1}^{6} R_j^{r_j}(\mathbf{x},t)B_j^{b_j}(\mathbf{x},t)[1-N_j(\mathbf{x},t)]^{1-r_j-b_j}, \\ B_i' &= \textstyle\sum_{s,s'} b_i' A \prod_{j=1}^{6} R_j^{r_j}(\mathbf{x},t)B_j^{b_j}(\mathbf{x},t)[1-N_j(\mathbf{x},t)]^{1-r_j-b_j}. \end{aligned} \tag{3.8}$$

The corresponding probabilities for the input state can be written

$$\begin{aligned} R_i &= \textstyle\sum_{s} r_i \prod_{j=1}^{6} R_j^{r_j}(\mathbf{x},t)B_j^{b_j}(\mathbf{x},t)[1-N_j(\mathbf{x},t)]^{1-r_j-b_j}, \\ B_i &= \textstyle\sum_{s} b_i \prod_{j=1}^{6} R_j^{r_j}(\mathbf{x},t)B_j^{b_j}(\mathbf{x},t)[1-N_j(\mathbf{x},t)]^{1-r_j-b_j}, \end{aligned} \tag{3.9}$$

which, using equation 3.3, can be written

$$\begin{aligned} R_i &= \textstyle\sum_{s,s'} r_i A \prod_{j=1}^{6} R_j^{r_j}(\mathbf{x},t)B_j^{b_j}(\mathbf{x},t)[1-N_j(\mathbf{x},t)]^{1-r_j-b_j}, \\ B_i &= \textstyle\sum_{s,s'} b_i A \prod_{j=1}^{6} R_j^{r_j}(\mathbf{x},t)B_j^{b_j}(\mathbf{x},t)[1-N_j(\mathbf{x},t)]^{1-r_j-b_j}. \end{aligned} \tag{3.10}$$

This leads to equations for the change in occupation probabilities due to collision:

$$\begin{aligned} R_i' - R_i &= \textstyle\sum_{s,s'} (r_i' - r_i) A \prod_{j=1}^{6} R_j^{r_j}(\mathbf{x},t)B_j^{b_j}(\mathbf{x},t)[1-N_j(\mathbf{x},t)]^{1-r_j-b_j}, \\ B_i' - B_i &= \textstyle\sum_{s,s'} (b_i' - b_i) A \prod_{j=1}^{6} R_j^{r_j}(\mathbf{x},t)B_j^{b_j}(\mathbf{x},t)[1-N_j(\mathbf{x},t)]^{1-r_j-b_j}. \end{aligned} \tag{3.11}$$

To address perturbations from an equilibrium distribution, I define a state density d, such that it is the mean occupancy of a state at lattice position $\mathbf{x}$. Thus

$$\begin{aligned} d_r(\mathbf{x}) &= \tfrac{1}{6}\textstyle\sum_{i=1}^{6} R_i(\mathbf{x}), \\ d_b(\mathbf{x}) &= \tfrac{1}{6}\textstyle\sum_{i=1}^{6} B_i(\mathbf{x}). \end{aligned} \tag{3.12}$$

Following the treatment of viscosity by Hénon [14], I consider a state close to isotropy:

$$\begin{aligned} R_i &= d_r(\mathbf{x}) + \nu_i(\mathbf{x}), \\ B_i &= d_b(\mathbf{x}) + \mu_i(\mathbf{x}), \end{aligned} \tag{3.13}$$

where the variations ν_i and μ_i are small. For an isotropic density distribution $\nu_i = \mu_i = 0$ for all i. As a consequence of equation 3.12,

$$\sum_{i=1}^{6} \nu_i(\mathbf{x}) = 0, \qquad \sum_{i=1}^{6} \mu_i(\mathbf{x}) = 0. \tag{3.14}$$

We substitute these equations into the equations for probability evolution 3.11, and then linearise in the small quantities μ and ν. Suppressing the argument $\mathbf{x}$, and following the algebra for the case of the red particles,

$$\begin{aligned}
\nu_i' - \nu_i &= \textstyle\sum_{s,s'}(r_i' - r_i)A\prod_{j=1}^{6}(d_r+\nu_j)^{r_j}(d_b+\mu_j)^{b_j}(1-d_r-d_b-\nu_j-\mu_j)^{1-r_j-b_j} \\
&= \textstyle\sum_{s,s'}(r_i' - r_i)A\prod_{i=j}^{6} d_r^{r_j} d_b^{b_j}(1-d_r-d_b)^{1-r_j-b_j} \\
&\qquad (1+\tfrac{\nu_j}{d_r})^{r_j}(1+\tfrac{\mu_j}{d_b})^{b_j}(1-(\tfrac{\nu_j+\mu_j}{1-d_r-d_b}))^{1-r_j-b_j} \\
&= \textstyle\sum_{s,s'}(r_i' - r_i)A\prod_{j=1}^{6} d_r^{r_j} d_b^{b_j}(1-d_r-d_b)^{1-r_j-b_j} \\
&\qquad (1+\tfrac{\nu_j}{d_r}r_j+\tfrac{\mu_j}{d_b}b_j-(\tfrac{\nu_j+\mu_j}{1-d_r-d_b})(1-r_j-b_j))+O(\nu^2,\mu^2,\nu\mu) \\
&\approx \textstyle\sum_{s,s'}(r_i' - r_i)Ad_r^{\Sigma r_j} d_b^{\Sigma b_j}(1-d_r-d_b)^{\Sigma(1-r_j-b_j)} \\
&\qquad (1+\textstyle\sum_{j=1}^{6}[\tfrac{\nu_j}{d_r}r_j+\tfrac{\mu_j}{d_b}b_j-(\tfrac{\nu_j+\mu_j}{1-d_r-d_b})(1-r_j-b_j)]) \\
&\approx \textstyle\sum_{s,s'}(r_i' - r_i)Ad_r^{p_r} d_b^{p_b}(1-d_r-d_b)^{(6-p_r-p_b)} \\
&\qquad (1+\textstyle\sum_{j=1}^{6}[\tfrac{\nu_j}{d_r}r_j+\tfrac{\mu_j}{d_b}b_j-(\tfrac{\nu_j+\mu_j}{1-d_r-d_b})(1-r_j-b_j)]).
\end{aligned} \tag{3.15}$$

Using 3.3 and 3.4 we recognise that

$$\sum_{s,s'}(r_i' - r_i)A = \sum_{s'} r_i' - \sum_{s} r_i = 0. \tag{3.16}$$

as the summations are over the same set of states, and so identical. Thus the first term in the expression cancels. Rearranging and using 3.14, the second term reduces to

$$\begin{aligned}
\nu_i' - \nu_i &= \sum_{s,s'}(r_i' - r_i)Ad_r^{p_r-1} d_b^{p_b-1}(1-d_r-d_b)^{(5-p_r-p_b)} \\
&\qquad \sum_{j=1}^{6}[\nu_j(r_j d_b(1-d_b)+b_j d_r d_b)+\mu_j(b_j d_r(1-d_r)+r_j d_r d_b)].
\end{aligned} \tag{3.17}$$

The corresponding equation for the blue particles is almost identical:

$$\mu_i' - \mu_i = \sum_{s,s'}(b_i' - b_i)Ad_r^{p_r-1}d_b^{p_b-1}(1-d_r-d_b)^{(5-p_r-p_b)} \sum_{j=1}^{6}[\nu_j(r_jd_b(1-d_b)+b_jd_rd_b)+\mu_j(b_jd_r(1-d_r)+r_jd_rd_b)] \quad (3.18)$$

From these equations we identify the linearised collision operator. Previous workers have defined the updating of the lattice in terms of the action of the collision operator on the non-equilibrium probability distribution (see for example [20] [21] [4]) by the equation

$$N_i(\mathbf{x}+\mathbf{c}_i, t+1) = N_i(\mathbf{x},t) + \sum_{j=1}^{6}\Omega_{ij}N_j^{neq}(\mathbf{x},t) \quad (3.19)$$

where N_j^{neq} is the non-equilibrium component of N_j. We identify a state vector $\mathbf{v}$ analogous to $\mathbf{N}^{neq}$ as

$$\mathbf{v} = (\nu_1, \mu_1, \nu_2, \mu_2, \ldots, \nu_6, \mu_6)^T. \quad (3.20)$$

As the equilibrium component is by definition constant with time, this defines a collision equation

$$v_i' - v_i = \sum_{j=1}^{12}\Omega_{ij}v_j \quad (3.21)$$

where the elements of the matrix Ω are given from 3.17 and 3.18 as

$$\begin{aligned}
\Omega_{2i-1,2j-1} &= \textstyle\sum_{s,s'}(r_i'-r_i)Ad_r^{p_r-1}d_b^{p_b-1}(1-d_r-d_b)^{(5-p_r-p_b)}(r_jd_b(1-d_b)+b_jd_rd_b),\\
\Omega_{2i-1,2j} &= \textstyle\sum_{s,s'}(r_i'-r_i)Ad_r^{p_r-1}d_b^{p_b-1}(1-d_r-d_b)^{(5-p_r-p_b)}(b_jd_r(1-d_r)+r_jd_rd_b),\\
\Omega_{2i,2j-1} &= \textstyle\sum_{s,s'}(b_i'-b_i)Ad_r^{p_r-1}d_b^{p_b-1}(1-d_r-d_b)^{(5-p_r-p_b)}(r_jd_b(1-d_b)+b_jd_rd_b),\\
\Omega_{2i,2j} &= \textstyle\sum_{s,s'}(b_i'-b_i)Ad_r^{p_r-1}d_b^{p_b-1}(1-d_r-d_b)^{(5-p_r-p_b)}(b_jd_r(1-d_r)+r_jd_rd_b).
\end{aligned} \quad (3.22)$$

DERIVATION OF THE DIFFUSION COEFFICIENT FOR A GENERALISED COLLISION OPERATOR

Having motivated the discussion by demonstrating the existence of the linearised collision operator for the two colour local system, we will now ignore all dependence on a particular set of collision rules and consider a general collision operator Ω_{ij}. This

has the advantage that we can consider a continuum of models, many of which are unachievable by defining collision rules, without reference to the particular microscopic dynamics, but still macroscopically realising the Navier-Stokes equations.

Whereas in the preceding discussion, we considered a state vector

$$s = (r_1, b_1, r_2, b_2, \ldots, r_6, b_6), \tag{3.23}$$

we now consider evolution of non equilibrium fluctuations in the probability distribution

$$\mathbf{v} = (\nu_1, \mu_1, \nu_2, \mu_2, \ldots, \nu_6, \mu_6). \tag{3.24}$$

We consider the matrix in 2x2 sub matrices ω_{ij} as motivated by equations 3.22. Following [27], we note that the collision operator must be six fold rotationally invariant and symmetric under exchange of directions in order for the collision to be isotropic. For $1 \leq i, j \leq 6$, we may write $\omega_{ij} = \omega_{|i-j|}$. We therefore denote the sub matrices by ω°, $\omega^{6\circ}$ etc, where the superscript is the angle in degrees between the directions. The full form of the operator is now

$$\Omega = \begin{pmatrix} \omega^{\circ} & \omega^{60} & \omega^{120} & \omega^{180} & \omega^{120} & \omega^{60} \\ \omega^{60} & \omega^{\circ} & \omega^{60} & \omega^{120} & \omega^{180} & \omega^{120} \\ \omega^{120} & \omega^{60} & \omega^{\circ} & \omega^{60} & \omega^{120} & \omega^{180} \\ \omega^{180} & \omega^{120} & \omega^{60} & \omega^{\circ} & \omega^{60} & \omega^{120} \\ \omega^{120} & \omega^{180} & \omega^{120} & \omega^{60} & \omega^{\circ} & \omega^{60} \\ \omega^{60} & \omega^{120} & \omega^{180} & \omega^{120} & \omega^{60} & \omega^{\circ} \end{pmatrix} \tag{3.25}$$

This matrix can be seen to be block circulant. The relevant mathematics of these structures is outlined in Appendix A.

We require that the operator satisfy certain necessary conservation rules; of each colour of particle and of uncoloured momentum. The total change in red mass at a site is given by

$$\sum_{i=1}^{6}(\nu_i' - \nu_i) = \sum_{i,j=1}^{6} \Omega_{ij} v_j, \tag{3.26}$$

where $\mathbf{v}$ is an arbitrary state vector. From conservation of this is required to be zero for all $\mathbf{v}$. We can write this condition

$$\sum_{i,j=1}^{6} w_i \Omega_{ij} v_j = 0, \tag{3.27}$$

where $\mathbf{w}$ is defined

$$[1,0,1,0,\ldots,1,0]. \tag{3.28}$$

Thus $\mathbf{w}$ is a left eigenvector of Ω with eigenvalue zero. From the conservation of blue mass, the same is also required of

$$[0,1,0,1,\ldots,0,1]. \tag{3.29}$$

This leads to four conservation equations as follows:

$$\omega_{11}^{0} + 2\omega_{11}^{60} + 2\omega_{11}^{120} + \omega_{11}^{180} = 0 \tag{3.30}$$

$$\omega_{12}^{0} + 2\omega_{12}^{60} + 2\omega_{12}^{120} + \omega_{12}^{180} = 0 \tag{3.31}$$

$$\omega_{21}^{0} + 2\omega_{21}^{60} + 2\omega_{21}^{120} + \omega_{21}^{180} = 0 \tag{3.32}$$

$$\omega_{22}^{0} + 2\omega_{22}^{60} + 2\omega_{22}^{120} + \omega_{22}^{180} = 0 \tag{3.33}$$

Conservation of momentum is similar. We require the total momentum vectors

$$\begin{aligned} &[c_{11}, c_{11}, \ldots, c_{61}, c_{61}], \\ &[c_{12}, c_{12}, \ldots, c_{62}, c_{62}], \end{aligned} \tag{3.34}$$

to be left eigenvectors with eigenvalue 0. By referring to Figure 3-1 these are written

$$[1,1,\cos(\pi/3),\cos(\pi/3),\cos(2\pi/3),\cos(2\pi/3),\ldots,\cos(5\pi/3),\cos(5\pi/3)], \tag{3.35}$$

$$[0,0,\sin(\pi/3),\sin(\pi/3),\sin(2\pi/3),\sin(2\pi/3),\ldots,\sin(5\pi/3),\sin(5\pi/3)]. \tag{3.36}$$

Choosing suitable linear combinations, these can be written

$$\begin{aligned} &[1,1,e^{\pi i/3},e^{\pi i/3},e^{2\pi i/3},e^{2\pi i/3},e^{\pi i},e^{\pi i},e^{4\pi i/3},e^{4\pi i/3},e^{5\pi i/3},e^{5\pi i/3}], \\ &[1,1,e^{-\pi i/3},e^{-\pi i/3},e^{-2\pi i/3},e^{-2\pi i/3},e^{-\pi i},e^{-\pi i},e^{-4\pi i/3},e^{-4\pi i/3},e^{-5\pi i/3},e^{-5\pi i/3}]. \end{aligned} \tag{3.37}$$

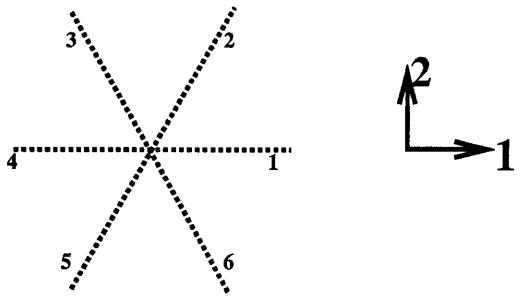

FIG. 3-1. Definition of lattice directions

Referring to equation A.12 these are seen to be legitimate left eigenvectors of the collision operator. The rotational isotropy of the lattice means that conservation of momentum in one direction implies conservation of momentum in all directions. Hence only two more conservation equations are generated:

$$\omega_{11}^{0} + \omega_{11}^{60} - \omega_{11}^{120} - \omega_{11}^{180} + \omega_{21}^{0} + \omega_{21}^{60} - \omega_{21}^{120} - \omega_{21}^{180} = 0, \tag{3.38}$$

$$\omega_{12}^{0} + \omega_{12}^{60} - \omega_{12}^{120} - \omega_{12}^{180} + \omega_{22}^{0} + \omega_{22}^{60} - \omega_{22}^{120} - \omega_{22}^{180} = 0. \tag{3.39}$$

We now analyse the macroscopic diffusive behaviour in terms of the eigenvalues and eigenvectors of the operator. In analogy to the calculation by Hénon [14] of the dynamic viscosity of the lattice, we establish a linear colour gradient which produces a uniform flux of colour at constant mass density. We define microscopic momentum fields for each colour:

$$M_{\alpha}^{r} = \sum_{i} R_i c_{i\alpha}, \qquad M_{\alpha}^{r} = \sum_{i} R_i c_{i\alpha}, \tag{3.40}$$

where α represents one of the two orthogonal directions 1 and 2, defined in Figure 3-1. We define the colour gradient to be in the x_2 direction, magnitude Q. This leads to

$$\begin{aligned} M_1^r &= M_1^b = 0, \\ M_1^r &= -M_2^b = M, \end{aligned} \tag{3.41}$$

where M is a constant (dependent on Q) to be determined. We postulate spatial variation for R_i and B_i of no higher order than linear, and so write

$$\begin{aligned} R_i &= d_r(\mathbf{x}) + \kappa_i x_2 + \epsilon_i, \\ B_i &= d_b(\mathbf{x}) + \eta_i x_2 + \delta_i. \end{aligned} \tag{3.42}$$

$d_r(\mathbf{x})$ and $d_b(\mathbf{x})$ are defined in equations 3.12. Due to the imposed colour gradient, and the requirement for uniform density,

$$\begin{aligned} d_r(\mathbf{x}) &= d_{r0} + \tfrac{Q}{6} x_2, \\ d_b(\mathbf{x}) &= d_{b0} - \tfrac{Q}{6} x_2. \end{aligned} \tag{3.43}$$

Homogeneity of total mass distribution requires

$$\begin{aligned} \textstyle\sum_{i=1}^{6} \kappa_i + \eta_i &= 0, \\ \textstyle\sum_{i=1}^{6} \epsilon_i + \delta_i &= 0. \end{aligned} \tag{3.44}$$

From equations 3.41 we get

$$\begin{aligned} \textstyle\sum_{i=1}^{6} \kappa_i c_{i1} &= 0, & \textstyle\sum_{i=1}^{6} \eta_i c_{i1} &= 0, \\ \textstyle\sum_{i=1}^{6} \kappa_i c_{i2} &= 0, & \textstyle\sum_{i=1}^{6} \eta_i c_{i2} &= 0, \\ \textstyle\sum_{i=1}^{6} \epsilon_i c_{i1} &= 0, & \textstyle\sum_{i=1}^{6} \delta_i c_{i1} &= 0, \\ \textstyle\sum_{i=1}^{6} \epsilon_i c_{i2} &= M, & \textstyle\sum_{i=1}^{6} \delta_i c_{i2} &= -M. \end{aligned} \tag{3.45}$$

We now compute the steady state velocity distribution which will produce a simple colour gradient. The propagation equation from one time step to the next can be written

$$R_i(\mathbf{x} + \mathbf{c}_i, t+1) = R_i'(\mathbf{x}, t), \tag{3.46}$$

with a similar equation for B_i. By assuming a steady state over time, this reduces to

$$R_i(\mathbf{x} + \mathbf{c}_i) = R_i'(\mathbf{x}). \tag{3.47}$$

Substituting from 3.13 for R and using 3.42 and 3.43, we obtain

$$\nu_i(\mathbf{x}) - \nu_i'(\mathbf{x}) = -(\kappa_i + Q/6) c_{i2} \tag{3.48}$$

with a similar equation for μ. Combining with the collision equation 3.21 leads to the coupled equations

$$\begin{array}{rcrcrcl} \sum_j[\Omega_{2i-1,2j-1}(\kappa_j x_2+\epsilon_j) & + & \Omega_{2i-1,2j}(\eta_i x_2+\delta_j)] & - & (\kappa_i+Q/6)c_{i2} & = & 0, \\ \sum_j[\Omega_{2i,2j-1}(\kappa_j x_2+\epsilon_j) & + & \Omega_{2i,2j}(\eta_i x_2+\delta_j)] & - & (\eta_i-Q/6)c_{i2} & = & 0. \end{array} \tag{3.49}$$

These equations must hold for all values of x_2. Solving for the coefficients of x_2, we postulate a common functional form for κ_i and η_i:

$$\begin{aligned} \kappa_i &= K_1 c_{i1} + K_2 c_{i2} \\ \eta_i &= H_1 c_{i1} + H_2 c_{i2}. \end{aligned} \tag{3.50}$$

Note that constant terms, as employed by Hénon [14] in the equivalent section of his development, could be absorbed into the external gradient, as they do not cause anisotropy. These forms satisfy equations 3.44, and from equations 3.45, we find $K_1 = K_2 = H_1 = H_2 = 0$. Thus $\kappa_i = \eta_i = 0$, so equations 3.49 can be written

$$\begin{array}{rcrcrcl} \sum_j[\Omega_{2i-1,2j-1}\epsilon_j & + & \Omega_{2i-1,2j}\delta_j] & - & \frac{Q}{6}c_{i2} & = & 0 \\ \sum_j[\Omega_{2i,2j-1}\epsilon_j & + & \Omega_{2i,2j}\delta_j] & + & \frac{Q}{6}c_{i2} & = & 0 \end{array} \tag{3.51}$$

Defining two vectors

$$\mathbf{y} = (\epsilon_1, \delta_1, \ldots, \epsilon_6, \delta_6), \tag{3.52}$$

$$\mathbf{z} = (c_{12}, -c_{12}, \ldots, c_{62}, -c_{62})^T, \tag{3.53}$$

we can write these equations in vector form:

$$\Omega\mathbf{y} = \frac{Q}{6}\mathbf{z}. \tag{3.54}$$

By writing $\mathbf{z}$ as a linear combination of the right eigenvectors of Ω the problem is reduced to a eigen problem.

It remains to determine the values of ϵ_i and δ_i. We make an ansatz that $\mathbf{y}$ is a scalar multiple of $\mathbf{z}$. This is a valid solution only if the vector $\mathbf{z}$ is an eigenvector of the operator Ω with a non zero eigenvalue. If the operator is non-defective (the eigenvectors span the twelve space on which they are defined), it is unique to within

an arbitrary linear combination of null eigenvectors. This satisfies equation 3.44, and from equations 3.45 we derive the scaling to be $M/6$. Hence the equilibrium distribution can be written:

$$\begin{aligned} R_i &= d_{r0} + \tfrac{Q}{6}x_2 + \tfrac{M}{6}c_{i2}, \\ B_i &= d_{b0} - \tfrac{Q}{6}x_2 - \tfrac{M}{6}c_{i2}. \end{aligned} \tag{3.55}$$

This gives a relation for the ratio of the anisotropy in the velocity distribution to the applied colour gradient:

$$\frac{M}{Q} = \frac{1}{\lambda} \tag{3.56}$$

where λ is the eigenvalue of Ω corresponding to the eigenvector $\mathbf{z}$.

Note that each sub matrix ω has four elements, making a total of 16 variables. There are 8 distinct eigenvalues, (4 eigenvectors have distinct eigenvalues and 4 eigenvector pairs are made degenerate by the symmetry of the operator), which define the rate of damping of perturbations from equilibrium. The other degrees of freedom are absorbed into the eigenvectors. Thus there are many possible operators which give the same value for the transport properties. To achieve some simplification of this degeneracy, we look at the subset of operators which map to collisions in which the physical outcome of particle location is not affected by the colour. This makes the operators directly comparable to the discrete particle models in Chapter 2. The mathematics involved is discussed in Appendix B. This constraint leads automatically to the conservation relations for colour and momentum, and also requires that the vector $\mathbf{z}$ in equation 3.53 is indeed a right eigenvector for the operator. Thus for such a subclass, the preceding analysis is valid. Note that this condition on the dynamics is sufficient but not necessary - other sets of eigenvectors can also include the diffusivity eigenvector and satisfy the conservation relations.

For a simple concentration gradient, we expect the flow of colour to obey Fick's law [23]:

$$J = -D\frac{d\sigma}{dx}, \tag{3.57}$$

where J is the colour flux across a line per unit length, σ is the colour area density and D is the diffusion coefficient. The area of lattice corresponding to one lattice point is $\frac{\sqrt{3}}{2}$, so colour per unit area is $\frac{2}{\sqrt{3}}$ times colour per lattice point. Some care must be taken with measuring the flux. Following McNamara [22] and others, I calculate the flux crossing a line between two rows of lattice points, as shown previously in Figure 2-1. I define the measurement to take place after propagation and before collision. Thus to determine the flux resulting from a given colour gradient I measure the flux that has crossed the measurement line during the previous time step. Referring to Figure 3-1 for the appropriate directions,

$$J = R_2(\mathbf{x}+\mathbf{c}_2) - B_2(\mathbf{x}+\mathbf{c}_2) + R_3(\mathbf{x}+\mathbf{c}_3) - B_3(\mathbf{x}+\mathbf{c}_3) - R_5(\mathbf{x}) + B_5(\mathbf{x}) - R_6(\mathbf{x}) + B_6(\mathbf{x}) \tag{3.58}$$

Using the steady state populations, the density gradient of (red - blue) in the x_2 direction is $4Q/\sqrt{3}$, and

$$J = 2M/\sqrt{3} + Q/\sqrt{3}. \tag{3.59}$$

Hence the diffusion coefficient is defined

$$D = -\frac{M}{2Q} - \frac{1}{4}. \tag{3.60}$$

Using equation 3.56, we can write this in terms of the relevant eigenvalue of the collision operator:

$$D = -\frac{1}{2\lambda} - \frac{1}{4}. \tag{3.61}$$

A remark on the values of the numerical constants in this relation is in order. Clearly, they do not depend on the form of the collision operator, as this dependence is carried by the value of λ. Thus they are solely parameters of the lattice type. It is also worth noting the correspondence between $\frac{1}{\lambda}$ here and the constant γ used by Rothman and Zaleski [24], which has been defined by Zaleski [personal communication] as "the susceptibility of the gas to an imposed gradient". Different numerical constants are caused by the addition of a rest particle.

NUMERICAL EXPERIMENTS

From equation 3.12 I define a mean uncoloured state density

$$d(\mathbf{x}) = d_r(\mathbf{x}) + d_b(\mathbf{x}). \tag{3.62}$$

I assume variations in this quantity are first order small, as a result of the assumption of homogeneity of mass. I linearise about a local equilibrium which is derived by Fermi-Dirac statistics and has been given by a number of workers (eg. [25]):

$$T_i^{eq} = d_T(1 + \frac{\Delta d}{d_0} + 2c_{i\alpha}v_\alpha + G(d_0)Q_{i\alpha\beta}v_\alpha v_\beta) \tag{3.63}$$

where d_0 is the average population density on the lattice, $\Delta d = d - d_0$ and

$$\begin{aligned} G(d_0) &= 2\left(\tfrac{1-2d_0}{1-d_0}\right) \\ Q_{i\alpha\beta} &= c_{i\alpha}c_{i\beta} - \tfrac{1}{2}\delta_{\alpha\beta}. \end{aligned} \tag{3.64}$$

T represents either R or B. Note that this is the same equation as used by Gunstensen et al [4] without rest particles and with a prefactor for each colour. This is the equilibrium derived from the Fermi-Dirac statistics of the lattice-gas formulation. It has been widely recognised that this is not Galilean invariant. For the Boltzmann formulation this can be overcome by setting $G(d_0)$ to 1, but I chose to use the traditional equilibrium as it does not affect the measurement of diffusivity, and it allows a closer correspondence to the particle models.

I have produced an operator based upon the eigenvalue equations. Of the eight independent eigenvalues, three are defined zero by the conservation relations, and one controls the diffusivity. The other four I set to -1, as this immediately damps out non-equilibrium fluctuations in these eigenvector directions. I measure diffusivity as described in Chapter 2.

The reproducibility of the calculations is to within 1 part in 1000. I have confirmed that the diffusivity depends only on the relevant eigenvalue and not on its eigenvector. Figure 3-2 is a plot of diffusion coefficient against $1/\lambda$, and confirms the values

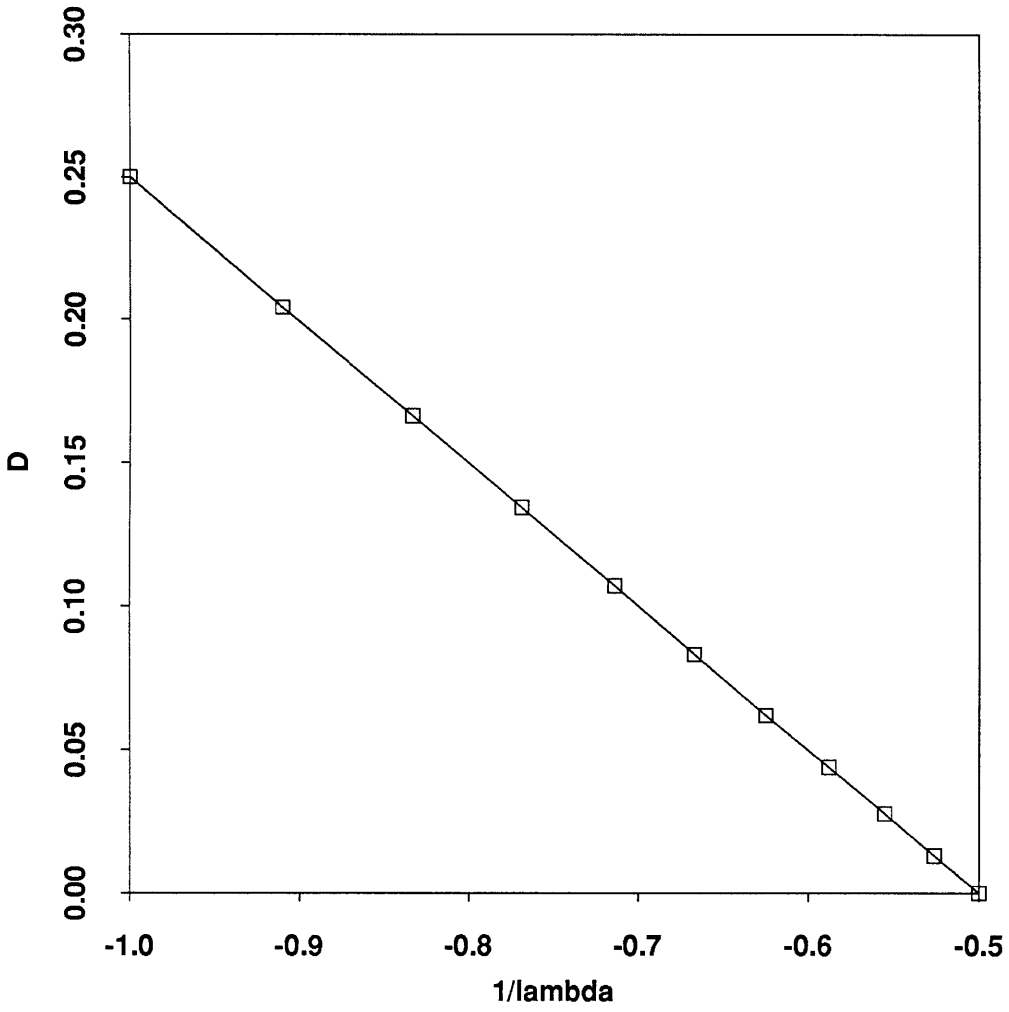

FIG. 3-2. Numerical confirmation of diffusivity eigenvalue relation.
Plot is D against $\frac{1}{\lambda}$, and therefore should have both gradient and x intercept of $-\frac{1}{2}$. This is as shown. Error bars are smaller than the symbols used to mark the data points.

calculated for the numerical constants in the diffusivity relation 3.61.

A naive treatment of the formula would suggest the development of negative diffusivity below -2. However, the collision operator is only stable for eigenvalues between 0 and -2 - simple linear stability theory shows that outside this region non equilibrium fluctuations tend to grow rather than be damped. This has been confirmed numerically. Figure 3-3 shows that the model obeys the theory well up to an eigenvalue of about -1.95, which corresponds to a diffusivity of 7.27×10^{-3} lattice units squared per time step. Below that the results deviate from prediction, suggesting computational instability.

In conclusion, we have developed a two colour collision operator which is capable of achieving low but bounded diffusivities with extremely good numerical confidence. Below this the linear theory developed may no longer hold. Thus it is likely that the linearised collision operator is no longer valid. To achieve very low diffusivity, we must turn to a non local model. This is described in Chapter 4.

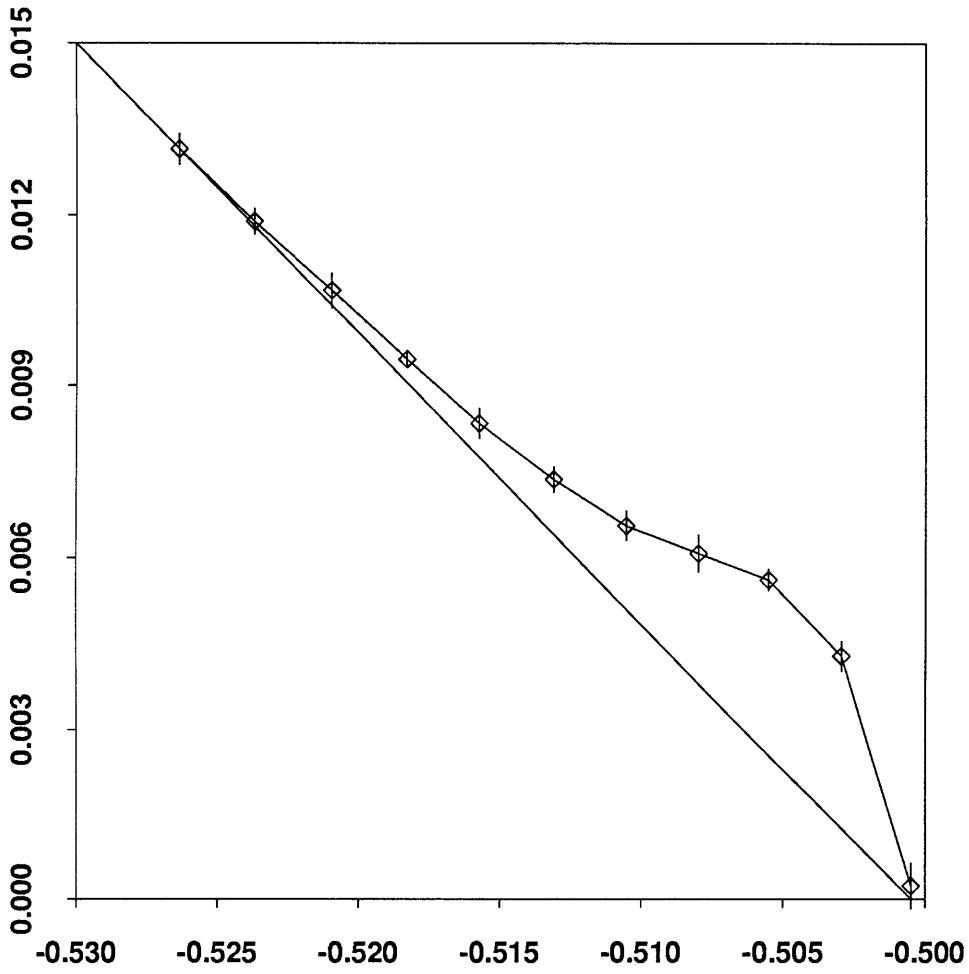

FIG. 3-3. Divergence from linear relationship at low diffusivities.

Straight line is theoretical relationship. Error bars are at the 1σ level.

Chapter 4

Towards a Lower Diffusivity Lattice-Boltzmann Model

In the previous chapters I have considered a low diffusivity lattice-gas model designed to preserve interfaces, and a Boltzmann formulation for a low-diffusivity lattice gas with local collision rules. I now combine these ideas to try to attain a lower diffusivity than was possible using the theory outlined in Chapter 3. The basis for this follows directly as a trivial special case of the lattice-Boltzmann model for immiscible fluids developed by Gunstensen et al. [4].

Essentially, the procedure followed in this model is the same as used in Chapter 2. We collide the particles ignoring colour using a one-phase linearised collision operator, developed in previous studies [21, 27]. We then reassign the colour by the equivalent rules based on local colour field, to align the colour at the site with the local colour gradient. All the "redness" is assigned to those sites closest to the surrounding concentration of red fluid, while all the "blueness" is apportioned to those sites closest to concentrations of blue fluid. As the colour and mass are fractional rather than discrete quantities, phase separation is far more efficient than for the particle model. Areas of fluid which are initially homogeneous remain so, with stable interfaces. A stable state forms from an initially random distribution of colour, consisting of homo-

geneous bubbles a few lattice units across. This is analogous to the equilibrium state of the particle model, but forms much more quickly, and is not subject to fluctuations. Hence the characteristic diffusivity of the model is zero.

The aim of this study is to produce models with very low finite diffusivity. To this end, I combine the zero diffusivity model with the local linearised operator described in Chapter 3. I define a number p between 0 and 1, such that a fraction p of the colour at each site is reassigned according to the zero-diffusivity model, and a fraction $1 - p$ according to the local model. Thus setting $p = 0$ gives the local model, and $p = 1$ the zero diffusivity model.

Diffusivity was measured for values of p from 0 to 1. The local model is considered at the limit of its applicability (diffusivity eigenvalue of -1.95) so as to minimise the amount of the zero-diffusivity model required and therefore also pathological effects it may cause. Figure 4-1 shows values obtained at low p. The negative values are an artifact of short run times, and will eventually approach zero. At higher values of p the zero diffusivity totally dominates the random rearrangement, and the net diffusivity is zero. Thus the algorithm is only interesting for low diffusivity systems for $p < 0.001$, when the measured diffusivity is small and positive. In physical terms, this is the regime when the influence of the non-local model is too weak for phase separation. These preliminary results clearly indicate a significant reduction in diffusivity. However, further studies are necessary to determine the stability of this combination and to ascertain that the behaviour is Fickian.

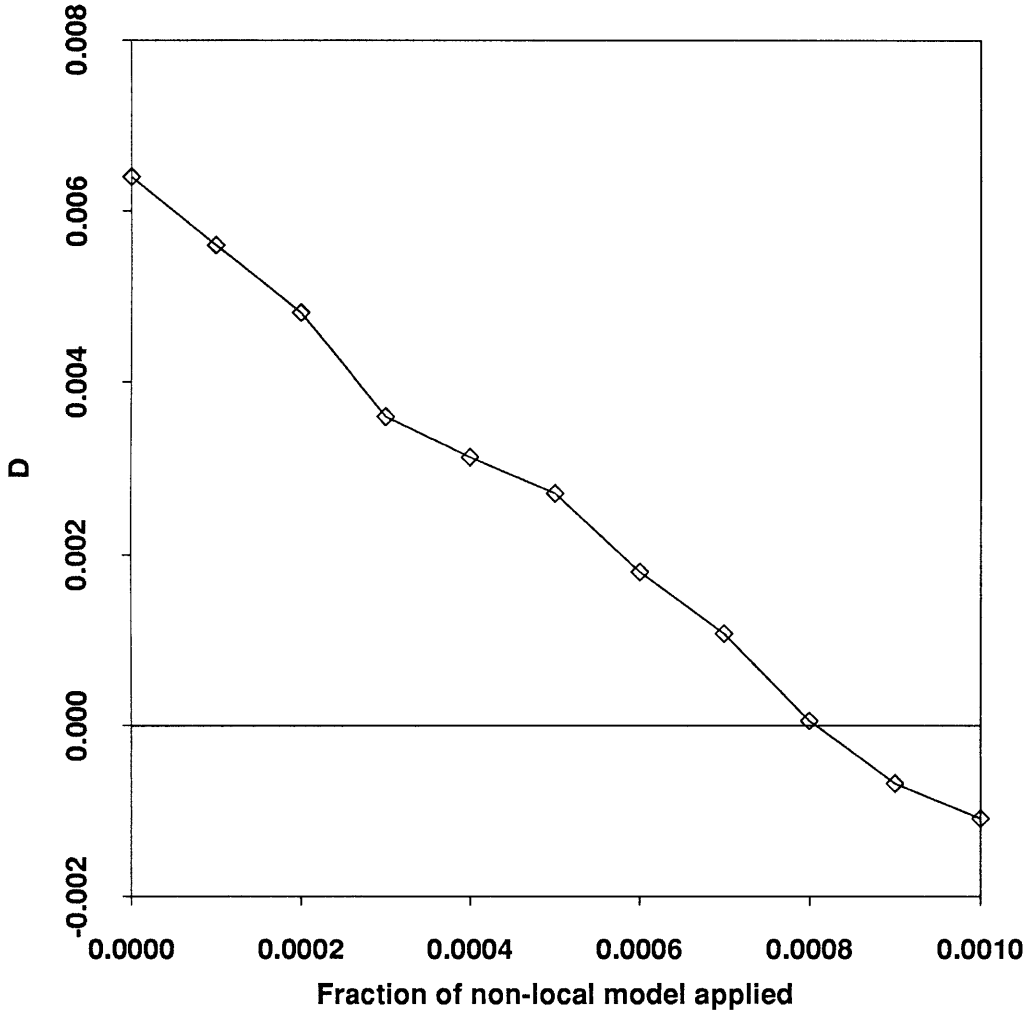

FIG. 4-1. Mixed model behaviour.

Chapter 5

Conclusions

The approaches presented here each have advantages over previous work in the field of low-diffusivity lattice gases. The non-local lattice gas developed in Chapter 2 was demonstrated to produce lower diffusivities than achieved before. The non-equilibrium fluctuations of the model are such that it will not be useful for studying simple low-diffusivity systems, but could have application to specialised flows.

The lattice-Boltzmann model developed in Chapter 3 is directly comparable to the previous lattice-gas work (the particular collision operators can be calculated for a given algorithm), shows much cleaner numerical behaviour and is much more easy to manipulate to achieve new physics. Further characterisation of the operator is necessary in order to define other transport coefficients in terms of the eigenvalue set, and to determine what effect the choice of eigenvectors has on the macroscopic physics. However, this model will be useful for the simulation of mixing mechanics over a large range of possible diffusivities.

Chapter 4 shows that it may be possible to reduce the lower limit of the diffusivity of the local operator by the addition of a very small amount of a non-local model. While this must be further characterised to confirm that, for example, Fickian behaviour is realised, this seems to offer hope of increasing even further the parameter range which can be simulated by the technique.

Appendix A

Circulant Matrices

We define an n x n circulant matrix **A** as

$$\mathbf{A} = \begin{pmatrix} a_0 & a_1 & a_2 & \dots & a_{n-1} \\ a_{n-1} & a_0 & a_1 & \dots & a_{n-2} \\ a_{n-2} & a_{n-1} & a_0 & \dots & a_{n-3} \\ \vdots & \vdots & \vdots & & \vdots \\ a_1 & a_2 & a_3 & \dots & a_0 \end{pmatrix} \tag{A.1}$$

Each row is equal to the previous row right shifted by one element. Such a matrix can be defined on a basis of simple shift operators $\mathbf{\Gamma}_i$. $\mathbf{\Gamma}_1$ is written

$$\mathbf{\Gamma}_1 = \begin{pmatrix} 0 & 1 & 0 & 0 & \dots & 0 \\ 0 & 0 & 1 & 0 & \dots & 0 \\ 0 & 0 & 0 & 1 & \dots & 0 \\ \vdots & \vdots & \vdots & \vdots & & \vdots \\ 1 & 0 & 0 & 0 & \dots & 0 \end{pmatrix} \tag{A.2}$$

We define $\mathbf{\Gamma}_i = \mathbf{\Gamma}_1^i$, so that, for example,

$$\mathbf{\Gamma}_2 = \begin{pmatrix} 0 & 0 & 1 & 0 & \dots & 0 \\ 0 & 0 & 0 & 1 & \dots & 0 \\ 0 & 0 & 0 & 0 & \dots & 0 \\ \vdots & \vdots & \vdots & \vdots & & \vdots \\ 0 & 1 & 0 & 0 & \dots & 0 \end{pmatrix} \tag{A.3}$$

and

$$\mathbf{\Gamma}_i^n = \mathbf{I}, \tag{A.4}$$

where $\mathbf{I}$ is the n x n identity matrix. It follows that the eigenvalues λ_k (k=0 to n-1) of all the matrices $\mathbf{\Gamma}_i$ are given by the nth complex roots of unity. Thus

$$\lambda_k = \exp(2\pi ik/n). \tag{A.5}$$

From this it is easy to show that the right eigenvectors of all the matrices $\mathbf{\Gamma}_i$ are given by the set of vectors

$$\mathbf{v}_k = [1, \lambda_k, \lambda_k^2, \lambda_k^3, \dots, \lambda_k^{n-1}]^T, \tag{A.6}$$

and the left eigenvectors by the set

$$\mathbf{u}_k = [1, \lambda_{n-k}, \lambda_{n-k}^2, \lambda_{n-k}^3, \dots, \lambda_{n-k}^{n-1}]. \tag{A.7}$$

Writing

$$\mathbf{A} = a_0\mathbf{I} + \sum_{i=1}^{n-1} a_i\mathbf{\Gamma}_i \tag{A.8}$$

it is clear that these are also the eigenvectors of the circulant matrix, independent of the individual elements a_i.

We now extend this analysis to block circulant matrices, that is matrices of the form

$$\mathbf{B} = \begin{pmatrix} \mathbf{A}_0 & \mathbf{A}_1 & \mathbf{A}_2 & \dots & \mathbf{A}_{n-1} \\ \mathbf{A}_{n-1} & \mathbf{A}_0 & \mathbf{A}_1 & \dots & \mathbf{A}_{n-2} \\ \mathbf{A}_{n-2} & \mathbf{A}_{n-1} & \mathbf{A}_0 & \dots & \mathbf{A}_{n-3} \\ \vdots & \vdots & \vdots & & \vdots \\ \mathbf{A}_1 & \mathbf{A}_2 & \mathbf{A}_3 & \dots & \mathbf{A}_0 \end{pmatrix} \tag{A.9}$$

where the $\mathbf{A}_i$ are square matrices of dimension m x m, making the overall matrix of dimension mn x mn. The following can be generalised for non-square sub blocks (see, for example, [28]), but this is not required here. Making use of the matrix Kronecker product, we can write this in the form

$$\mathbf{B} = \mathbf{I} \otimes \mathbf{A}_0 + \sum_{i=1}^{n-1} \mathbf{\Gamma}_i \otimes \mathbf{A}_i. \tag{A.10}$$

By analogy with the simple circulant matrices, and setting m equal to two, we seek right eigenvectors of the form

$$\mathbf{v}_k = ([1, \lambda_k, \lambda_k^2, \lambda_k^3, \ldots, \lambda_k^{n-1}] \otimes [p, q])^T, \tag{A.11}$$

and left eigenvectors

$$\mathbf{u}_k = [1, \lambda_{n-k}, \lambda_{n-k}^2, \lambda_{n-k}^3, \ldots, \lambda_{n-k}^{n-1}] \otimes [r, s]. \tag{A.12}$$

$[p, q]$ and $[r, s]$ are respectively the right and left eigenvectors of $\sum_{i=0}^{n-1} \mathbf{A}_i \exp(2\pi ik/n)$, and in general will not be eigenvectors of the individual matrices $\mathbf{A}_i$ unless all possess a common eigenvector. Hence, the eigenvalue problem is reduced from a 2n x 2n determinant to n 2 x 2 determinants of the form

$$|\sum_{i=0}^{n-1} \mathbf{A}_i \exp(2\pi ik/n) - \lambda \mathbf{I}| = 0. \tag{A.13}$$

Further details on circulant matrices can be found in reference [29].

Appendix B

The Collision Operator for Collisions Independent of Colour

Consider each submatrix of the linearised collision operator acting upon each two unit section of the perturbation vector. If we ignore colour we can compress this to a scalar multiplication. We require that this multiplication should not depend on the relative quantities of red and blue perturbation, only on their sum.

Consider the element (ν_i, μ_i) acted upon by the submatrix ω_{ij}:

$$\begin{pmatrix} \omega_{11} & \omega_{12} \\ \omega_{21} & \omega_{22} \end{pmatrix} \begin{pmatrix} \nu_i \\ \mu_i \end{pmatrix} = \begin{pmatrix} \omega_{11}\nu_i & + & \omega_{12}\mu_i \\ \omega_{21}\nu_i & + & \omega_{22}\mu_i \end{pmatrix} \tag{B.1}$$

Thus for the scalar representation to be colourblind, we require $(\omega_{11}+\omega_{21})\nu_i+(\omega_{12}+\omega_{22})\mu_i$ to be a multiple of $\nu_i+\mu_i$. This implies

$$\omega_{11}+\omega_{21}=\omega_{12}+\omega_{22} \tag{B.2}$$

We can rewrite ω in a more symmetric form:

$$\omega = \begin{pmatrix} r+t & s+t \\ s-t & r-t \end{pmatrix} \tag{B.3}$$

where r, s and t are arbitrary numbers. This matrix has eigenvalues

$$\lambda = r \pm s \tag{B.4}$$

with corresponding right eigenvectors

$$(s+t, s-t)^T, \qquad (1,-1)^T, \tag{B.5}$$

and left eigenvectors

$$(1,1), \qquad (t-s, t+s). \tag{B.6}$$

We now construct the full collision operator from matrices of this form. As all the submatrices have the left eigenvector $(1,1)$ and the right eigenvector $(1,-1)^T$ in common, these are solutions to the eigen problem formulated in equation A.13. Thus the operator has a set of six right eigenvectors

$$\mathbf{v}_k = ([1, \lambda_k, \lambda_k^2, \lambda_k^3, \ldots, \lambda_k^{N-1}] \otimes [1,-1])^T, \tag{B.7}$$

and six left eigenvectors

$$\mathbf{v}_k = [1, \lambda_{N-k}, \lambda_{N-k}^2, \lambda_{N-k}^3, \ldots, \lambda_{N-k}^{N-1}] \otimes [1,1]. \tag{B.8}$$

corresponding to the other set of eigenvalues. The left set include the eigenvectors required for the momentum conservation equations 3.35 and 3.36, while the right set include the eigenvectors required to define the diffusivity 3.53. Thus an operator with such sub blocks fulfills all the necessary conditions for the analysis in Chapter 3 to hold.

Bibliography

[1] D. H. Rothman, Geophysics **53** 509 (1988).

[2] A. Cancelliere, C. Chang, E. Foti, D.H. Rothman, and S. Succi, Physics of Fluids A **2** 2085 (December 1990).

[3] A. K. Gunstensen and D. H. Rothman, Physica D **15** in press (1990).

[4] A. K. Gunstensen, D. H. Rothman, S. Zaleski, and G. Zanetti, Phys. Rev. A. **15** *in press* (1991).

[5] E. Guyon, J.-P. Nadal, and Y. Pomeau, editors *Disorder and Mixing* Kluwer Academic (1988).

[6] G. F. Davis, Mantle dynamics In D. E. James, editor, *The Encyclopedia of Solid Earth Geophysics* 806 Van Nostrand Reinhold (1989).

[7] H. K. Moffatt, Liquid metal mhd and the geodynamo In *Proc. IATAM Symposium on Liquid Metal Magnetohydrodynamics, Riga, USSR, May 1988* Kluwer Academic (in press).

[8] J. Hardy, O. de Pazzis, and Y. Pomeau, Phys. Rev. A. **13** 1949 (1976).

[9] U. Frisch, B. Hasslacher, and Y. Pomeau, Phys. Rev. Lett. **56** 1505 (1986).

[10] U. Frisch, D. d'Humières, B. Hasslacher, P. Lallemand, Y. Pomeau, and J.-P. Rivet, Complex Systems **1** 648 (1987).

[11] S. Wolfram, J. Stat. Phys. **45** 471 (1986).

[12] D. d'Humières, P. Lallemand, and U. Frisch, Europhys. Lett. **2** 291 (1986).

[13] D. d'Humières, P. Clavin, P. Lallemand, and Y. Pomeau, Y. Comp. Rend. Acad. Sci. Paris **II 303** 1169 (1986).

[14] M. Hénon, Complex Systems **1** 763-789 (1987).

[15] D. H. Rothman, J. Stat. Phys. **56** 1119 (1989).

[16] D. d'Humières, P. Lallemand, J. P. Boon, D. Dab, and A. Noullez, Fluid dynamics with lattice gases In R. Livi, S. Ruffo, S. Cilberto, and M. Buiatti, editors, *Chaos and Complexity* 278 World Scientific Singapore (1988).

[17] D. H. Rothman and J. Keller, J. Stat. Phys. **52** 1119 (1988).

[18] C. Appert, D.H. Rothman, and S. Zaleski, Physica D **15** in press (1990).

[19] A. K. Gunstensen and D. H. Rothman, Physica D **15** in press (1990).

[20] G. McNamara and G. Zanetti, Phys. Rev. Lett. **61(20)** 2332 (1988).

[21] F. Higuera and J. Jimenez, Europhysics Letters **9(7)** 663 (1989).

[22] G. R. McNamara, Europhys. Lett. **12(4)** 329 (1990).

[23] R. P. Feynman, R. B. Leighton, and M. Sands, *The Feynman Lectures on Physics* volume 1 Addison-Wesley (1963).

[24] D. H. Rothman and S. Zaleski, Journal de Physique **50** 2161 (1989).

[25] C. Burges and S. Zaleski, Complex Systems **1** 31 (1987).

[26] R. L. Liboff, *Introduction to the Theory of Kinetic Equations* Wiley (1969).

[27] F. Higuera, S. Succi, and R. Benzi, Europhysics Letters **9(4)** 345 (1989).

[28] J. E. Wall, *Control and estimation for large-scale systems having spatial symmetry* PhD thesis Massachusetts Institute of Technology August 1978.

[29] P. J. Davis, *Circulant Matrices* Wiley New York (1979).